

Heterogeneity of Alveolar Macrophages in Experimental Silicosis

by Steven Hildemann,¹ Claus Hammer,¹ and Fritz Krombach¹

The alveolar macrophage (AM) population has been shown to be heterogeneous in composition as well as in function. The aim of our study was to assess morphological and functional features of AM in an experimental model of quartz-induced lung fibrosis by flow cytometric methods. Twelve cynomolgus monkeys were exposed 8 hr/day, 5 days/week for 26 months to either normal atmosphere ($n = 5$) or 5 mg/m^3 DQ12 $< 5 \mu\text{m}$ quartz dust ($n = 7$). After 20 months of exposure, we studied AM phagocytosis by incubating bronchoalveolar lavage cells with fluorescent polystyrene microspheres (mean diameter $1.91 \mu\text{m}$). Using a fluorescence-activated cell sorter analyzer, AM subpopulations were identified via their volume/side scatter properties. After selective electronic "gating" of the AM populations, both the percentage of phagocytic AM and the mean number of ingested microspheres per AM were determined. In addition, a phagocytic index (microspheres/AM \times % phagocytic AM $\times 10^{-3}$) and a hypothetical total phagocytic capacity of one lung (phagocytic index \times total number of AM $\times 10^{-6}$) were calculated. The total bronchoalveolar lavage cell counts rose ($75.6 \pm 11.3 \times 10^6$ versus $10.1 \pm 0.8 \times 10^6$) significantly after quartz exposure. In contrast, the percentage of phagocytic AM was significantly ($p < 0.05$) reduced ($43.5 \pm 5.0\%$ versus $74.2 \pm 1.4\%$). Flow cytometric measurements revealed the appearance of an AM subpopulation characterized by size/granularity features identical to blood monocytes. Only minimal numbers of these cells were found under normal conditions, but they constituted 50% of the entire AM population in the quartz group. Selective analysis of these AM subpopulations demonstrated a quartz-induced reduction of phagocytosis within the subpopulation of large AM ($69.0 \pm 4.8\%$ versus $85.8 \pm 4.9\%$), whereas the comparatively low phagocytic activity of smaller, monocyte-like AM was slightly elevated ($16.2 \pm 2.1\%$ versus $10.9 \pm 1.7\%$). High numbers of these relatively inactive cells led to a decreased phagocytic index (8.6 ± 1.7 versus 16.2 ± 2.3) that was, however, more than compensated for by the higher total AM numbers, leading to an enhanced pulmonary phagocytic capacity (403.6 ± 85.2 versus 137.6 ± 16.5). We conclude from these results that chronic quartz exposure causes a shift from large, active (with respect to phagocytosis) AM to small, monocyte-like, less active AM. This effect is likely to be responsible for the relatively impaired phagocytic activity of the total AM population. Nevertheless, the total pulmonary phagocytic capacity is enhanced in quartz-exposed animals due to increased total AM numbers.

Introduction

Alveolar macrophages (AM) play a central role in the pathogenesis of interstitial lung diseases such as silicosis (1). Aside from acting as the primary nonspecific defense of the lung against inhaled particulate matter, AM have been shown to modulate the inflammatory response by secreting a variety of mediators (2–5). Recent studies have suggested, however, that AM may be a heterogeneous population of several distinct subpopulations with respect to morphological, functional, and biochemical aspects (6–9). The aim of this study was to assess several morphological and functional features of AM in an experimental model of quartz-induced lung fibrosis using flow cytometric methods. We present data demonstrating that long-term intermittent inhalation exposure to quartz in nonhuman primates leads to a change in the composition of the AM population. We found two characteristic subpopulations of AM with unique morphological appearances and phagocytic capabilities.

¹Institute for Surgical Research, Ludwig-Maximilians-University, Munich, Germany.

Address reprint requests to F. Krombach, Institut für Chirurgische Forschung, Klinikum Grobhadern, Marchioninstr. 15, 8000 München 70, Germany.

Materials and Methods

Animals and Exposure Conditions

We separated 12 cynomolgus monkeys (*Macaca fascicularis*) with a body weight of 3–6 kg into two groups. In exposure-free intervals, the animals were kept in spacious steel cages under natural daylight. A standard primate chop-diet, additional fruit supplement, and water were supplied *ad libitum*. The two groups of animals received an intermittent inhalation exposure regimen of 8 hr/day and 5 days/week for 26 months except for public holidays and a 1-week rest after open lung biopsies. For exposure, the animals were placed in 7.5-m^3 capacity inhalation chambers featuring controlled climatic conditions (25°C temperature, 70% relative humidity). The first group (control group) was sham-exposed to clear, normobaric air. The second group (quartz-exposed group) received a concentration of 5 mg/m^3 of DQ12 standard quartz dust (10). Temperature, humidity, and respirable dust concentration were monitored and controlled continuously. The concentration of airborne respirable dust was measured with a digital photometer (TM digital μP , Hund GMBH, Wetzlar, FRG). The photometer reading was calibrated

in terms of mass concentration of respirable dust by means of a gravimetric dust sampler (11).

Experimental Protocol

After a 12-month acclimatization and control phase, the total exposure time lasted 26 months. During this period, the animals were exposed according to the conditions listed above. Bronchoalveolar lavage (BAL) was performed at bimonthly intervals along with open lung biopsies after 12 and 18 months. After cessation of exposure, various radiological, pathohistological, and pulmonary function examinations were performed (12). The flow cytometric data presented demonstrate the results of 20 months of exposure.

Bronchoalveolar Lavage

We performed BAL procedures as described previously (13). Briefly, the animals were anesthetized by an intramuscular injection of 15 mg/kg ketamine (Ketanest; Parke, Davis & Co., Munich, FRG) and 2 mg/kg xylazine (Rompun, Bayer, Leverkusen, FRG). With the animal in a supine position, a flexible fiberoptic bronchoscope (BF P10, Olympus, Munich, FRG) was wedged into the main bronchus of the left lung. The entire left lung was washed with 100 mL of sterile 0.9% saline at room temperature in five aliquots of 20 mL. Fluid was withdrawn applying moderate suction and gathered in 10-mL Falcon vials. Consecutive samples were immediately filtered through sterile gauze, pooled in 50-mL conical centrifuge tubes, and centrifuged at room temperature for 10 min at 300g. The supernatant was aspirated and the cell pellet resuspended in phosphate-buffered saline (PBS). Total cell yield was determined using a Coulter counter (Coulter Electronics GMBH, Krefeld, FRG) and cell viability assessed using trypan blue exclusion. Cytochrome smears served to identify the cellular populations stained with May-Grünwald-Giemsa and toluidine blue. The percentage of alveolar macrophages, lymphocytes, neutrophils, eosinophils, and mast cells was determined by counting 300 cells by light microscopy.

Preparation of Alveolar Macrophages

We adjusted BAL cells to a density of 1×10^6 cells/mL in RPMI 1640 medium containing 20% fetal calf serum. We placed 1 mL of the cell suspension in 5-mL polypropylene centrifuge tubes and incubated them with 5×10^7 fluorescent monodispersed carboxylated polystyrene microspheres (1.91 μm in diameter; Polysciences, St. Goar, FRG) for 60 min at 37°C on a shaker platform. Phagocytosis was stopped by placing the tubes in icewater for 5 min. This was followed by two cycles of centrifugation (300g for 10 min), discarding the supernatant, resuspending in ice-cold PBS, and flow cytometric measurement.

Flow Cytometric Assay

Using a modified assay originally described by Steinkamp et al. (14), flow cytometric analyses were performed on a fluorescence-activated cell sorter Analyzer (Becton Dickinson, Mountain View, CA) equipped with a Hg-Cd arc lamp and using a standard FITC-PE filter pack providing an excitation wave-

length of 488 nm. A sample of cells was measured at a flow rate of 150 cells/sec. The data on volume, 90° light scatter, and fluorescence distribution properties of BAL cells were collected in list mode on a Consort 30 data handling system (Becton Dickinson). The AM subpopulations were selectively analyzed by electronic gating of volume-sidescatter dot-plots and fluorescence-distribution graphs. The graphs demonstrated a minimum of five to seven sharply defined fluorescence peaks (Fig. 1) rising in fluorescence intensity by a constant factor equivalent to the fluorescence intensity of one microsphere. These fluorescence peaks corresponding to cells with one, two, or more associated microspheres were separated by electronic markers to determine the percentage of phagocytic AM. The mean number of microspheres per AM was calculated by dividing the compounded fluorescence intensity in the AM gate by the fluorescence intensity of one single microsphere. From these data, a phagocytic index combining both parameters was calculated ($\text{microspheres/AM} \times \% \text{phagocytic AM} \times 10^{-2}$). The phagocytic index in turn allows for the calculation of a hypothetical total phagocytic capacity of one lung ($\text{phagocytic index} \times \text{total number of AM} \times 10^{-6}$).

Statistics

Results are expressed as means \pm standard error of the mean (SEM). Individual group comparisons were made using the Mann-Whitney *U*-test. Differences with $p < 0.05$ were considered statistically significant.

Results

All animals tolerated the exposure conditions well without apparent signs of indisposition during dust exposure. The body weight of the animals did not change significantly during the 26-month observation period.

Twenty months after the start of exposure, BAL fluid recovery remained unchanged among individual animals as well as between groups, with values of $75.3 \pm 1.5\%$ for the control and $78.2 \pm 2.1\%$ for the quartz-exposed group. Interestingly, cell viability did not differ significantly between the control (75.8 ± 2.6) and the quartz-exposed group (77.8 ± 2.0). There was, however, a dramatic increase of the total cell count in the quartz-exposed group. By 20 months after the start of quartz exposure, the total number of BAL cells rose by a factor of 7.5 in that group ($75.6 \pm 11.3 \times 10^6$) as compared to the control ($10.1 \pm 0.8 \times 10^6$). This was accompanied by a change in the proportional distribution of BAL cells (Fig. 2). Differential cell counts showed a significant reduction in the percentage of AM ($67.2 \pm 4.4\%$ in the quartz-exposed group versus $86.3 \pm 2.6\%$ in the control) along with a relative increase in the percentage of neutrophils ($17.2 \pm 3.1\%$ in the quartz-exposed group, $1.7 \pm 0.4\%$ in the control). The lymphocyte population remained unchanged ($7.7 \pm 1.6\%$ in the quartz-exposed group versus $5.5 \pm 1.8\%$ in the control).

Figure 1 shows two characteristic volume-sidescatter dot-plots derived from flow cytometric measurement. Figure 1a demonstrates the normal picture of cells from a control animal featuring a homogeneous population of predominantly large cells with considerable granularity (as defined by light-scattering properties) corresponding to the AM population. In addition, a popula-

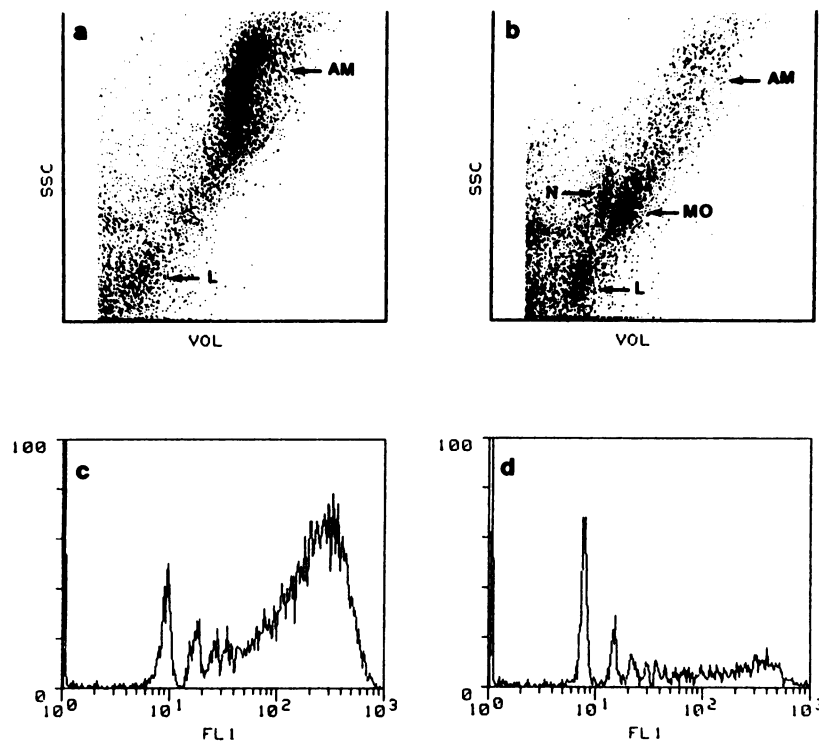


FIGURE 1. Flow cytometrically obtained volume-sidescatter dot-plots and fluorescence distribution graphs of bronchoalveolar lavage cells characteristic for a control (a and c) and a quartz-exposed animal (b and d) after incubation with fluorescent polystyrene microspheres. The letters indicate the respective cell populations: AM, large alveolar macrophages; MO, small, monocyte-like alveolar macrophages; L, lymphocytes; N, neutrophils. Graphs were taken using a gate including the entire AM population.

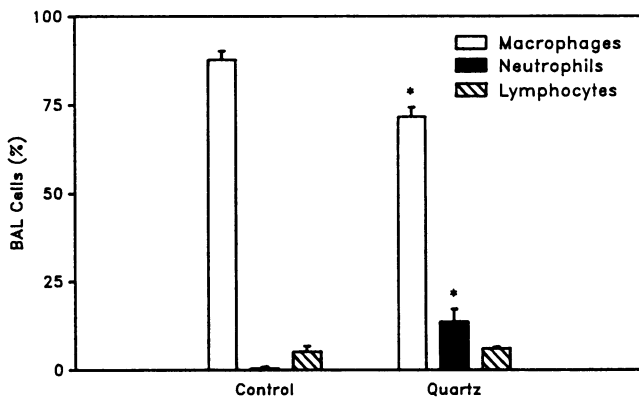


FIGURE 2. Bronchoalveolar lavage differential cell counts obtained 20 months after start of quartz exposure. Data are presented as means \pm SEM. Asterisk indicates a statistically significant difference from the control group ($p < 0.05$).

tion of few, small, and dense cells corresponding to lymphocytes and moderate amounts of debris are visible. Figure 1b, in contrast, shows the characteristic findings in a quartz-exposed animal. The population of AM is spread out and relatively reduced in number. Most striking, however, is the observation of two distinct subpopulations with individual volume and light-scattering features, i.e., a subpopulation of large, granulated AM along with a well-defined subpopulation of smaller, denser AM. These subfractions differed from one another with respect to

Table 1. Immune opsonin-independent phagocytosis parameters determined by flow cytometry.

Parameter	Mean \pm SEM	
	Control (n = 5)	Quartz (n = 7)
Phagocytic AM, %	74.2 \pm 1.4	43.5 \pm 5.0*
Mean number of microspheres per AM	21.5 \pm 2.5	18.7 \pm 2.4
Phagocytic large AM, %	85.8 \pm 4.9	69.0 \pm 4.8*
Phagocytic small AM, %	10.9 \pm 1.7	16.2 \pm 2.1*
Ratio small AM/large AM	0.2 \pm 0.1	1.0 \pm 0.1*
Phagocytic index	16.2 \pm 2.3	8.6 \pm 1.7*
Phagocytic capacity	137.6 \pm 16.5	403.6 \pm 85.2*

AM, alveolar macrophage.

* $p < 0.05$ versus control.

phagocytic activity (Table 1). In addition, neutrophils and lymphocytes, along with increased amounts of debris, are evident as compared to the control.

The corresponding fluorescence-distribution graphs (Fig. 1) were taken using a gate including the entire AM population. The logarithmic X-axis shows the distribution of cell-associated fluorescence divided into channels; the Y-axis shows the number of events in that channel. Figure 1c from a control animal demonstrates a moderate number of AM with one to four associated microspheres found in peaks one through four, followed, however, by high numbers of AM with five or more associated microspheres found in a single wide fluorescence peak. AM with as many as 40 associated microspheres were observed. Figure 1d from a quartz-exposed animal, in contrast, demonstrates increased numbers of AM with one or two

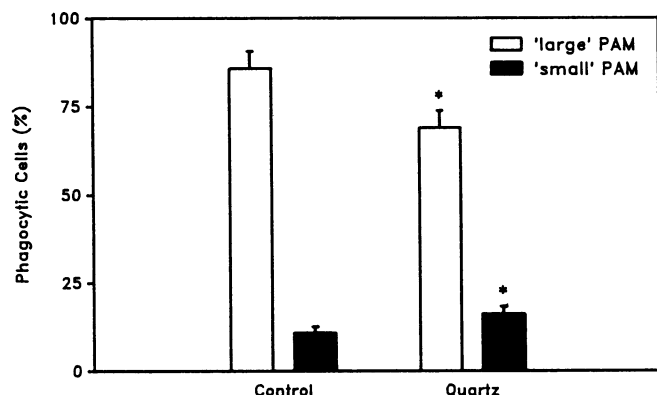


FIGURE 3. Phagocytic activity of large and small alveolar macrophages as determined by flow cytometric analysis. Data are presented as means \pm SEM. Asterisks indicate a statistically significant difference from the control group ($p < 0.05$).

associated microspheres, followed, however, by reduced numbers of cells with three to five associated microspheres. Cells with more than five associated microspheres, although evident, are drastically reduced in number. Overall, the percentage of phagocytic AM was significantly reduced in the quartz-exposed group ($43.5 \pm 5.0\%$) as compared to the control ($74.2 \pm 3.8\%$). The mean number of microspheres per AM taken across the entire population, however, was not significantly altered (Table 1). Neutrophil phagocytosis was negligible because in the quartz-exposed group the percentage of phagocytizing neutrophils was only $18.6 \pm 2.7\%$, and the mean number of particles was 1.5 ± 0.6 microspheres/neutrophil.

Looking at the individual AM subpopulations, it was evident that the amount of large, phagocytic AM was again significantly reduced in the quartz-exposed group as compared to the control. The phagocytic activity of small AM from quartz-exposed animals, however, proved to be significantly higher than that of control animals (Fig. 3). In addition, these cells were more numerous by a factor of 5 in the BAL of exposed animals, leading to a ratio of small AM versus large AM of 1.0 ± 0.1 in that group compared to 0.2 ± 0.1 in the control. The sum of these data was accounted for in a phagocytic index that was significantly reduced in the quartz-exposed group as compared to the control group. Under *in vivo* conditions, however, it must be considered that the total number of AM in the BAL rose 6-fold after intermittent inhalation exposure to quartz. Therefore, the overall phagocytic capacity of the lung rose significantly after silica exposure, compared to control values (Table 1).

Discussion

In this study, we have described changes in the composition of the AM population in an experimental model of quartz-induced lung fibrosis in the nonhuman primate. After intermittent inhalation exposure to quartz, we found two subpopulations of AM with distinct morphological features and phagocytic capabilities, as determined by flow cytometric methods.

The occurrence of silicosis as an occupational lung disease is currently underestimated (15). The cytotoxic effects of silica on macrophages have been well documented *in vitro* (16) and *in vivo*

(17). To study the *in vivo* effects of quartz exposure, we established a long-term inhalation exposure model of quartz-induced pulmonary fibrosis in the nonhuman primate. In contrast to the much-applied intratracheal instillation of quartz particles, we chose inhalation exposure for its more "physiological" qualities. The proportional distribution of BAL cells from our control group was in good agreement with the situation found by others in that species (18) as well as in the healthy human volunteer (19). In addition, we could demonstrate that in our experimental model, long-term serial BAL procedures, despite a repeatedly induced short-term neutrophil influx, led neither to chronic changes of the BAL cell profile nor to damage of the bronchoalveolar structures (20). After 20 months of quartz exposure, we found a dramatic increase in total cell counts, AM, and neutrophil numbers. Similar quartz-induced changes in the BAL cell profile have been reported in the mouse (21), the rat (22,23), the sheep (24), and the human (25).

Flow cytometry constitutes an improvement in the study of phagocytosis by allowing large numbers of cells to be sampled in a rapid, automated way. At the same time, data on the phagocytic activity of individual cells can be obtained (26,27). Furthermore, the technique has been used as an analytical approach for comparing the electro-optical characteristics of AM subpopulations (28–30). By using unopsonized polystyrene microspheres of uniform size, we combined these two advantages in an assay of opsonin-independent phagocytosis. AM, unlike phagocytes in other organs, are exposed to inorganic particles that do not generate an immune response (31). Recent studies suggest, however, that the pathway previously termed "non-specific" phagocytosis may be mediated by cell surface antigens (receptors?), the blocking of which leads to an inhibition of the phagocytic uptake of latex particles (32). Notably in silicosis, this pathway, which is distinct from immune opsonin-dependent phagocytosis, could be an important mechanism to remove such particles from the lung.

Our data demonstrate a significant depression of the phagocytic activity in the AM population as a whole after chronic *in vivo* exposure to silica. A dose-dependent inhibition of phagocytosis has been reported by others (33) after *in vitro* exposure of AM to silica. When differentiating among subpopulations of AM, however, this effect can be attributed to several factors: The phagocytic activity of large AM was indeed reduced, while this parameter was elevated among the fraction of small AM as compared to the control. Although the phagocytic activity of small AM, whose electro-optical characteristics are identical to those of blood monocytes (unpublished observation), increased after quartz-exposure, the activity of this population was still less (by a factor of 4) than that of normal, large AM. The observed shift in the ratio of large AM to small AM in favor of the latter must therefore affect the average performance of the subpopulation. This is reflected in the phagocytic index which reaches only 50% of the control values in the exposed group.

What causes the observed influx of small, monocyte-like AM into the alveoli? Conflicting views exist concerning the maintenance of AM in the normal lung. Kinetic studies of cell turnover in the AM population suggest that under normal conditions the predominant mechanism of AM production is the direct passage of blood monocytes across the interstitium into the alveolus (34). In contrast, recent studies reported that the AM

cell population is supported to a large extent by cellular proliferation *in situ* rather than direct monocyte influx from the blood compartment (35). During lung inflammation, however, monocyte influx has been shown to dramatically increase (36).

The morphological appearance of our cells would support this view. A facilitated passage could hypothetically be due to an increased expression of adhesion molecules by pulmonary microvascular endothelium. The existence of a wide variety of cytokines that modulate cellular interactions has already been established in the normal and diseased lung (2). Some of these mediators possess chemotactic activities that may play a substantial role in the development of silicosis by recruiting large numbers of inflammatory cells. The dramatic rise in the total AM numbers observed in this study could be explained in part by those mechanisms.

In summary, we conclude from these results that chronic quartz exposure causes a shift from large, active (with respect to phagocytosis) AM to small, monocyte-like, less active AM. Most likely this effect is responsible for the relatively impaired phagocytic activity of the total AM population. Nevertheless, the total phagocytic capacity of the lung is enhanced in quartz-exposed animals due to elevated total AM numbers.

The authors thank Anne-Marie Allmeling for her expertise and technical assistance. The study was supported in part by BMFT grant 01 VD 492/7.

REFERENCES

- Davis, G. S. Pathogenesis of silicosis: current concepts and hypotheses. *Lung* 164: 139-154 (1986).
- Kelley, J. State of the art: cytokines of the lung. *Am. Rev. Respir. Dis.* 141: 765-788 (1990).
- Fantone, J. C., Feltner, D. E., Brieland, J. K., and Ward, P. A. Phagocytic cell-derived inflammatory mediators and lung disease. *Chest* 91: 428-435 (1987).
- Driscoll, K. E., Lindenschmidt, R. C., Maurer, J. K., Higgins, J. M., and Ridder, G. Pulmonary response to silica or titanium dioxide: inflammatory cells, alveolar macrophage-derived cytokines, and histopathology. *Am. J. Respir. Cell. Mol. Biol.* 2: 381-390 (1990).
- Brown, G. P., Monick, M., and Hunninghake, G. W. Fibroblast proliferation induced by silica-exposed human alveolar macrophages. *Am. Rev. Respir. Dis.* 138: 85-89 (1988).
- Gant, V. A., and Hamblin, A. S. Human bronchoalveolar macrophage heterogeneity demonstrated by histochemistry, surface markers and phagocytosis. *Clin. Exp. Immunol.* 60: 539-545 (1985).
- Shellito, J., Kaltreider, H. B. Heterogeneity of immunologic function among subfractions of normal rat alveolar macrophages. II. Activation as determinant of functional activity. *Am. Rev. Respir. Dis.* 131: 678-683 (1985).
- Chandler, D. B., Fuller, W. C., Jackson, R. M., and Fulmer, J. D. Studies of membrane receptors and phagocytosis in subpopulations of rat alveolar macrophages. *Am. Rev. Respir. Dis.* 133: 461-467 (1986).
- Calhoun, W. J., and Salisbury, S. M. Heterogeneity in cell recovery and superoxide production in buoyant, density-defined subpopulations of human alveolar macrophages from healthy volunteers and sarcoidosis patients. *J. Lab. Clin. Med.* 114: 682-690 (1989).
- Robock, K. Standard quartz DQ12 < 5 μ m for experimental pneumoconiosis research projects in the federal republic of germany. *Ann. Occup. Hyg.* 16: 63-66 (1973).
- Armbruster, L., Breuer, H., Gebhart, J., and Neulinger, G. Photometric determination of respirable dust concentration without elutriation of coarse particles. *Part. Charact.* 1: 96-101 (1984).
- Krombach, F., Ronge, R., Hildemann, S., Fiehl, E., Wanders, A., Burkhardt, D., Allmeling, A., and Hammer, C. A model of experimental silicosis in a compressed air environment. In: *Surgical Research: Recent Concepts and Results* (A. Baethmann and K. Messmer, Eds.), Springer-Verlag, Berlin, 1987, pp. 59-68.
- Krombach, F., König, G., Wanders, A., Lersch, C., and Hammer, C. Effect of repeated bronchoalveolar lavage on free lung cells and peripheral leukocytes. *Transplant. Proc.* 17(5): 2134-2136 (1985).
- Steinkamp, J. A., Wilson, J. S., Saunders, G. C., and Stewart, C. C. Phagocytosis: Flow cytometric quantitation with fluorescent microspheres. *Science* 215: 64-66 (1982).
- Valiante, D. J., and Rosenman, K. D. Does silicosis still occur? *J. Am. Med. Assoc.* 262: 3003-3007 (1989).
- Allison, A. C., Harington, J. S., and Birbeck, M. An examination of the cytotoxic effects of silica on macrophages. *J. Exp. Med.* 124: 141-154 (1966).
- Takemura, T., Rom, W. N., Ferrans, V. J., and Crystal, R. G. Morphologic characterisation of alveolar macrophages from subjects with occupational exposure to inorganic particles. *Am. Rev. Respir. Dis.* 140: 1674-1685 (1989).
- Haley, P. J., Muggenburg, B. A., Rebar, A. H., Shopp, G. M., and Bice, D. E. Bronchoalveolar lavage cytology in cynomolgus monkeys and identification of cytologic alterations following sequential saline lavage. *Vet. Pathol.* 26: 265-273 (1989).
- Cherniak, R. M., Banks, d. E., Bell, D. Y., Davis, G. S., Hughes, J. M., and King, T. E. Bronchoalveolar lavage constituents in healthy individuals, idiopathic pulmonary fibrosis, and selected comparison groups. *Am. Rev. Respir. Dis.* 141(5): S167-S201 (1990).
- Krombach, F., König, G., Wanders, A., Fiehl, E., Riemüller, R., and Rosenbruch, M. Experimental studies on the effects of serial bronchoalveolar lavage (abstract). *Am. Rev. Respir. Dis.* 141(4): A891 (1990).
- Callis, A. H., Sohnle, P. G., Mandel, G. S., Wiessner, J., and Mandel, N. S. Kinetics of inflammatory and fibrotic pulmonary changes in a murine model of silicosis. *J. Lab. Clin. Med.* 105: 547-553 (1985).
- Davis, G. S., Hemenway, D. R., Evans, J. N., Lapenas, D. J., and Brody, A. R. Alveolar macrophage stimulation and population changes in silica-exposed rats. *Chest* 80: 8s-10s (1981).
- Struhar, D., Harbeck, R. J., and Mason, R. J. Lymphocyte populations in lung tissue, bronchoalveolar lavage fluid, and peripheral blood in rats at various times during the development of silicosis. *Am. Rev. Respir. Dis.* 139: 28-32 (1989).
- Bégin, R., Dufresne, A., Cantin, A., Possmayer, F., and Sébastien, P. Quartz exposure, retention and early silicosis in sheep. *Exp. Lung Res.* 15: 409-428 (1989).
- Bégin, R., Cantin, A. M., Boileau, R. D., and Bisson, G. Y. Spectrum of alveolitis in quartz-exposed human subjects. *Chest* 92: 1061-1067 (1987).
- Stewart, C. C., Lehnert, B. E., and Steinkamp, J. A. *In vitro* and *in vivo* measurement of phagocytosis by flow cytometry. *Methods Enzymol.* 132: 183-191 (1986).
- Parod, R. J., and Brain, J. D. Uptake of latex particles by macrophages: characterization using flow cytometry. *Am. J. Physiol.* 245 (Cell Physiol. 14): C220-C226 (1983).
- Lehnert, B. E., Valdez, Y. E., Fillak, D. A., Steinkamp, J. A., and Stewart, C. C. Flow cytometric characterization of alveolar macrophages. *J. Leukoc. Biol.* 39: 285-298 (1986).
- Kradin, R. L., McCarthy, K. M., Pfeffer, F. I., and Schneeberger, E. E. Flow cytometric and ultrastructural analysis of alveolar macrophage maturation. *J. Leukoc. Biol.* 40: 407-417 (1986).
- Dethloff, L. A., and Lehnert, B. E. Pulmonary interstitial macrophages: isolation and flow cytometric comparisons with alveolar macrophages and blood monocytes. *J. Leukoc. Biol.* 43: 80-90 (1988).
- Parod, R. J., and Brain, J. Immune opsonin-independent phagocytosis by pulmonary macrophages. *J. Immunol.* 136: 2041-2047 (1986).
- Parod, R. J., Godleski, J. J., and Brain, J. D. Inhibition of immune opsonin-independent phagocytosis by antibody to a pulmonary macrophage cell surface antigen. *J. Immunol.* 136: 2048-2054 (1986).
- Zimmerman, B. T., Canono, B. P., and Campbell, P. A. Silica decreases phagocytosis and bactericidal activity of both macrophages and neutrophils *in vitro*. *Immunology* 59: 521-525 (1986).
- Bowden, D. H., and Adamson, I. Y. R. Role of monocytes and interstitial cells in the generation of alveolar macrophages. I. Kinetic studies of normal mice. *Lab. Invest.* 42: 511-517 (1980).
- Shellito, J., Esparza, C., and Armstrong, C. Maintenance of the normal rat alveolar macrophage cell population. *Am. Rev. Respir. Dis.* 135: 78-82 (1987).
- Adamson, I. Y. R., and Bowden, D. H. Role of monocytes and interstitial cells in the generation of AMs: II. Kinetic studies after carbon loading. *Lab. Invest.* 42: 518-531 (1980).